Drug Design, Development and Therapy

Dovepress
Taylor & Francis Group

Open Access Full Text Article

ORIGINAL RESEARCH

The Effective Compound Combination of Bufei Yishen Formula III Improves the Mitochondrial Dysfunction via Inhibiting JNK/Sab Pathway in COPD Mice

Mengwei Song[1,2,*], Mi Han[1,2,*], Haoyu Zhang[1], Yifan Yang[1,2], Yange Tian[1,2], Jiansheng Li[2,3], Jie Zhao[1,2]

[1]Academy of Chinese Medical Sciences, Henan University of Chinese Medicine, Zhengzhou, 450046, People's Republic of China; [2]Henan Key Laboratory of Chinese Medicine for Respiratory Disease, Collaborative Innovation Center for Chinese Medicine and Respiratory Diseases Co-Constructed by Henan Province and Education Ministry of P.R. China, Henan University of Chinese Medicine, Zhengzhou, 450046, People's Republic of China; [3]Department of Respiratory Diseases, The First Affiliated Hospital of Henan University of Chinese Medicine, Zhengzhou, 450000, People's Republic of China

*These authors contributed equally to this work

Correspondence: Jie Zhao, Academy of Chinese Medical Sciences, Henan University of Chinese Medicine, 156 Jinshui East Road, Zhengdong, Zhengzhou, Henan, 450046, People's Republic of China, Tel +86-15100165967, Email Jiezhao1702@163.com

Purpose: The effective compound combination of Bufei Yishen formula III (ECC-BYF III) has shown protective effects against chronic obstructive pulmonary disease (COPD). However, its effect on mitochondrial dysfunction remains unclear. The current study aimed to investigate the effect of ECC-BYF III on mitochondrial dysfunction in COPD mice and elucidate its potential mechanisms.

Methods: Twenty-eight BALB/c mice were randomized into four groups: control, model, ECC-BYF III, and NAC (N-acetylcysteine) groups. A COPD model was established using cigarette smoke and Klebsiella pneumoniae for 8 weeks. The mice in the ECC-BYF III group were treated with ECC-BYF III (7.7 mg/kg/d), and the NAC group was treated with NAC (78 mg/kg/d) for eight weeks. Mice in the control and model groups were administered with 0.5% sodium carboxymethyl cellulose (25 mL/kg/d) for eight weeks. Then pulmonary function, histopathology, inflammatory factor levels, mitochondrial ultrastructure and function, and immunoblotting analyses were evaluated.

Results: Compared with the model, ECC-BYF III significantly improved the decline in pulmonary function and histopathological changes. Furthermore, ECC-BYF III ameliorated mitochondrial dysfunction by restoring the mitochondrial membrane potential, increasing mitochondrial complex I activity, and decreasing tumor necrosis factor-α (TNF-α) level and protein expressions of SH3BP5 (Sab), Phospho-JNK (P-JNK), and cleaved CASP3.

Conclusion: The results suggest that the potential therapeutic benefit of ECC-BYF III against mitochondrial dysfunction in COPD is due to the inhibition of the JNK/Sab pathway, which will help to further understand the potential mechanisms of ECC-BYF III in the treatment of COPD.

Keywords: chronic obstructive pulmonary disease, Chinese medicine, mitochondrion, apoptosis, JNK/Sab pathway

Introduction

Chronic obstructive pulmonary disease (COPD), a common chronic lung disease, is characterized by chronic respiratory symptoms and persistent airflow obstruction.[1] It has been reported that almost 10% of the global population over 40 years of age suffers from this disease, and its morbidity is still increasing.[2] Because of the high mortality, COPD has already been the third leading cause of death worldwide, causing enormous economic and social burdens. However, the recommended treatment options only could relieve the symptoms and improve the quality of life but fail to prevent

Received: 6 September 2024
Accepted: 5 January 2025
Published: 24 January 2025

Graphical Abstract

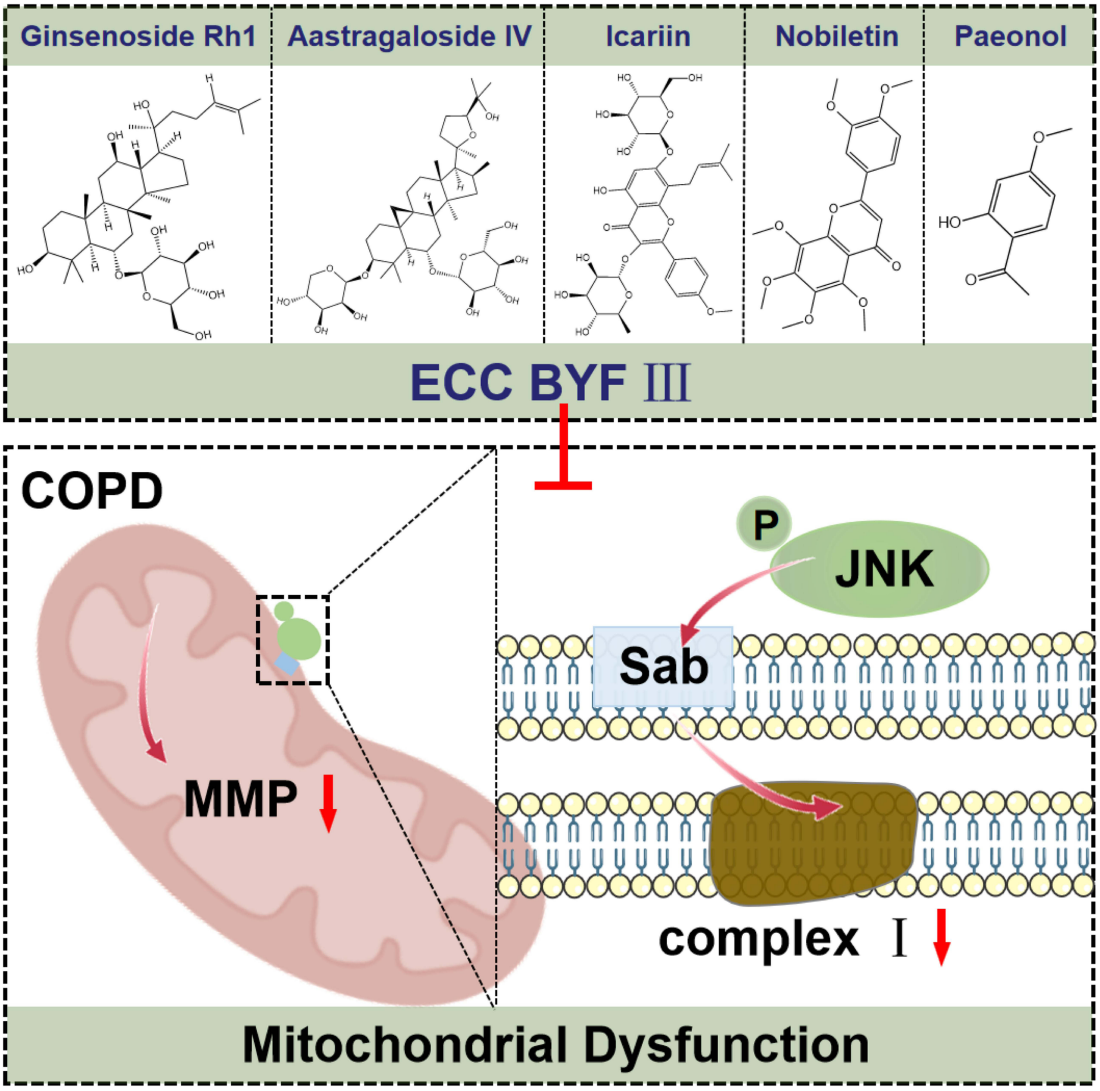

the progression of this disease. Therefore, finding targeted therapeutic drugs to prevent the development of COPD is necessary and urgent.

The development of COPD remains unclear, but cigarette smoking (CS) has been recognized as a critical driver.[3] CS contains a large number of toxic substances that stimulate mitochondria to produce excessive reactive oxygen species (ROS).[4,5] Accumulation of excessive ROS in the lung can affect mitochondrial function by decreasing mitochondrial membrane potential (MMP) and mitochondrial respiratory chain enzyme activity. Mitochondrial dysfunction finally leads to cell death and even tissue damages, which is a key inducer for the development of COPD.[6] It has been reported that restoring mitochondrial function could attenuate cell damages and improve the condition of COPD.[5,7] The mitochondrial membrane protein SH3 domain-binding protein 5 (Sab) is a kind of mitochondrial outer membrane scaffold protein, which can regulate mitochondrial physiological functions.[8] Recent studies have shown that Sab can associate with the c-Jun N-terminal kinase (JNK) and then cause mitochondrial ROS (mtROS) accumulation by disturbing mitochondrial electron transport chain, leading to mitochondrial dysfunction and cell death.[4] In addition, silencing Sab can inhibit sustained JNK activation and reduce mtROS production, thereby alleviating cell damage in mice.[8,9] Consequently,

inhibiting the JNK/Sab pathway to reduce mtROS production and alleviate mitochondrial dysfunction may be a new therapeutic approach to cure COPD.

The Bufei Yishen formula (BYF; Patent ZL.2011101175781), a traditional Chinese herbal formula, has been used clinically for many years to treat COPD.[10,11] Clinical studies have shown that BYF can improve patients' respiratory symptoms, reduce the frequency of exacerbations, and improve their quality of life. However, the complex composition of BYF (consisting of 12 Chinese medicinal herbs) makes it difficult to elucidate its underlying mechanism. Therefore, based on the new modern traditional Chinese medicine model of group-effect relationship and component compatibility optimization, BYF has been simplified and optimized to an effective compound combination of Bufei Yishen formula III (ECC-BYF III).[12] ECC-BYF III, a combination of five compounds consisting of 20(S)-Ginsenoside Rh1, astragaloside IV, icariin, nobiletin, and paeonol, is more favorable for elucidating its pharmacodynamic mechanism. Previous reports have confirmed that ECC-BYF III could improve pulmonary function and decrease oxidative stress on COPD rats.[13] However, its pharmacological mechanisms have not yet been clarified.

In this study, we established COPD model in mice, and evaluated the effects of ECC-BYF III on pulmonary function and pathology. In addition, we explored the underlying mechanisms of ECC-BYF III in improving mitochondrial dysfunction by inhibiting the JNK/Sab pathway. The results of this study may provide a theoretical basis for the clinical application of ECC-BYF III and a new approach for the treatment of COPD by targeting on mitochondrial dysfunction and JNK/Sab inhibitors.

Materials and Methods

Animals

In total, twenty-eight male BALB/C mice of SPF grade (age 6–8 weeks and weight 19.9 ± 0.9 g), were purchased from the Beijing Vital River Laboratory Animal Technology Co., Ltd. (China; SCXK(KY)2021-0006). All animal studies were approved by the Experimental Animal Care and Ethics Committee of the Henan University of Chinese Medicine (approval no. DWLL201903072).

Drugs and Reagents

ECC-BYF III is composed of 20(S)-Ginsenoside Rh1, icariin, paeonol, nobiletin, and astragaloside IV. 20(S)-Ginsenoside Rh1 was purchased from Chengdu Chroma-Biotechnology Co., Ltd. (Chengdu, China; CHB180608), and icariin, paeonol, and astragaloside IV were purchased from Chengdu Must Bio Technology Co., Ltd. (Chengdu, China; MUST-16111710, MUST-16071405, and MUST-17022804). Nobiletin was acquired from Xi'an Hui Lin Bio-Tech Co., Ltd. (Xi'an, China; HL-20170312). Prior to use, ECC-BYF III was completely dissolved in 0.5% sodium carboxymethyl cellulose (CMC-Na). N-acetylcysteine (NAC) was purchased from GLPBIO (Montclair, USA; GC11786). NAC was completely dissolved in 0.5% CMC-Na solution. Hongqi Canal® filter cigarettes were purchased from the Henan Tobacco Industry (Zhengzhou, China). Klebsiella pneumoniae (strain ID: 46117) was provided by the National Center for Medical Culture Collection (CMCC). The hematoxylin-eosin (HE) staining kit, mitochondrial membrane potential assay kit with JC-1, mitochondrial complex I/NADH-CoQ reductase activity assay kit and RIPA buffer were purchased from Beijing Solarbio Science & Technology Co., Ltd. (Beijing, China; G1080 and G1100, M8650, BC0515, and R0010). Mouse TNF-α (Tumor Necrosis Factor Alpha) ELISA kit was purchased from Elabscience Biotechnology Co., Ltd. (Wuhan, China; E-EL-M3063). Pierce BCA protein assay kit was purchased from Thermo Fisher Scientific (Waltham, USA; 23227). P-JNK, Sab, horseradish peroxidase-conjugated secondary antibodies (goat anti-rabbit IgG or goat anti-mouse IgG), and β-actin were purchased from Proteintech (Wuhan, China; 80024-1-RR, 11127-2-AP, SA00001-2, SA00001-1, and 66009-1-1g), and Cleaved CASP3 was purchased from Cell Signaling Technology (Boston, USA; 9664).

COPD Modeling, Grouping, and Drug Administration

We established a COPD model according to previous studies.[10] After one week of adaptive feeding, twenty-one mice were randomly selected to establish COPD mice. Another seven mice served as the control group. The COPD model mice were

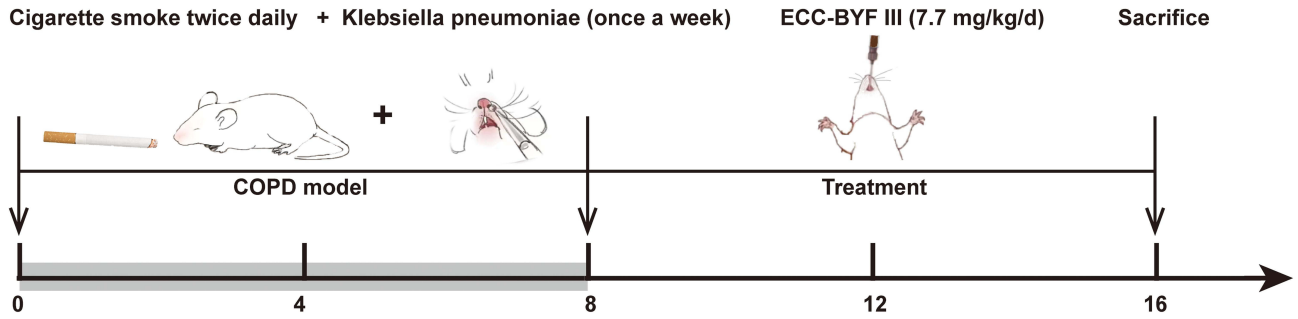

Figure 1 Schematic experimental design: COPD model preparation.

established by cigarette smoke and bacterial infection exposure during 8 weeks. In brief, the whole body of COPD model mice were exposed to CS (concentration: 3000 ± 500 ppm, twice daily, 40 min each time) in a cigarette smoke exposure system. Meanwhile, COPD mice were received an intranasal instillation of Klebsiella pneumoniae (5×10^6 CFU/mL, 20 μL/mouse) once a week for 8 weeks. The control group was reared under standard conditions, and received the same volume of normal saline solution. After that, COPD mice were randomly separated and divided into three groups with seven mice per group: the model group, ECC-BYF III group, and NAC group. From nine to sixteen weeks, the ECC-BYF III group was intragastrically administered with ECC-BYF III suspension (7.7 mg/kg/d), and the NAC group was intragastrically administered with NAC suspension (78 mg/kg/d). Mice in the control and model groups were intragastrically administered with 0.5% CMC-Na (25 mL/kg/d). After 16 weeks, mice were sacrificed (Figure 1).

Pulmonary Function

For unrestrained mice, tidal volume (VT), minute volume (MV), peak expiratory flow (PEF), and expiratory flow at 50% tidal volume (EF50) were evaluated using the whole-body plethysmograph (WBP) system (Buxco, NC, USA).

HE Staining

The 4% formalin-fixed lung tissues were dehydrated, embedded in paraffin, and cut into 4μm thickness. The sections were stained with hematoxylin and eosin (HE) for morphological evaluation. Morphological changes were observed using a light microscope (PM-10AD; Olympus Optical, Tokyo, Japan). Under a microscope (200×), a cross (+) was made under each visual field, and the total length of the cross (L) was measured. The numbers of alveolar septum (Ns) and alveoli (Na) and the area of the visual field (S) were obtained in the same visual field. Six visual fields were randomly taken in each slice. The mean alveolar number (MAN) and mean linear intercept (MLI) of the lung tissue were calculated according to the formulas MAN (/mm^2) =Na/S and MLI (μm) = L/Ns.

Transmission Electron Microscopy (TEM)

Lung tissues were cut into small pieces of approximately 1 mm^3 thickness and soaked in 2.5% glutaraldehyde fixative at 4 °C. Samples were examined by the electron microscope at the Center of Henan University of Chinese Medicine for observation of type II alveolar epithelial cells and mitochondrial ultrastructure.

Mitochondrial Membrane Potential (MMP)

MMP was determined using the mitochondrial membrane potential assay kit with JC-1 according to the manufacturer's instructions. In brief, fresh lung tissues (25 mg) were grinded in the DMEM complete medium with 10% FBS (1 mL) on ice and then centrifuged at 4 °C for 5 min at 3000 rpm. After removing the supernatant, red blood cell lysis buffer (1 mL) was added to the precipitate, lysed on ice for 10 min, and centrifuged at 4 °C for 5 min at 3000 rpm. Then the supernatant was removed, and the precipitate samples was used for the follow-up measurement. JC-1 working solution was then added into samples and incubated for 20 min at 37 °C. Then, JC-1 working solution was discarded by centrifugation followed by 3-time washing with 1× JC-1 incubation buffer. All samples were analyzed using a FACSCelesta™ flow

cytometer (BD, USA) after JC-1 staining. The percentages of fluorescence intensity of J-aggregates (with a specific red fluorescence emission maximum at 590 nm) were calculated.

Mitochondrial Complex I Activity

Mitochondrial Complex I activity was evaluated using the mitochondrial complex I/NADH-CoQ reductase activity assay kit following the manufacturer's instructions. Briefly, lung tissues (25 mg) were homogenized in the reaction buffer I (1 mL) using a homogenizer and then centrifuged at 4 °C for 10 min at 600 × g. The supernatants were collected in new centrifuge tubes, and then centrifuged at 4 °C for 15 min at 11,000 g. Then, 200 μL of reaction buffers I and II were added to the precipitates and ultrasonically broken (20% power, 5s of ultrasound, 10s intervals, repeated 15 times). Next, reagent I (154 μL), the working solution (20 μL) and reagent IV (16 μL) were added in a 96-well plate (UV plate), respectively. The mixture was mixed, and the absorbance values were measured at 340 nm by Microplate Reader (BIO-TEK, USA).

Enzyme Linked Immunoassay Assay ELISA

The levels of tumor necrosis factor-α (TNF-α) in the bronchial alveolar lavage fluid (BALF) and serum were measured using a mouse TNF-α ELISA kit, according to the manufacturer's instructions.

Western Blotting

Total proteins in lung tissues were extracted with RIPA buffer. The lysates were centrifuged at 4 °C for 15 min at 12,000 rpm, the supernatants were collected, and the concentrations of proteins were measured using the BCA protein assay kit. Samples were electrophoresed on sodium dodecyl sulphate polyacrylamide gel electrophoresis (SDS-PAGE) gels, and then the proteins were transferred to 0.22 μm polyvinylidene fluoride (PVDF) membranes for 90 min. After that, membranes were blocked with 5% non-fat milk for 1 h at room temperature. The membranes were incubated with primary antibodies (1:1000; P-JNK, Sab, cleaved CASP3, and β-actin) overnight at 4 °C, and then incubated with secondary antibody (1:2000; anti-rabbit and anti-mouse) for 1 h at room temperature. The protein bands were immersed in an enhanced chemiluminescence solution and observed using a Touch Imager (e-BLOT, China). The internal reference β-actin was used as a control.

Molecular Docking

Molecular docking was performed using AutoDock Vina (Docking number = 10) to elucidate the binding mechanism between JNK1 (Protein Data Bank (PDB) ID: 4QTD) and five effective compounds from Chinese herbal medicine including 20(S)-Ginsenoside Rh1, icariin, paeonol, nobiletin and astragaloside IV. The 3D structure of 20 (S)-Ginsenoside Rh1 was downloaded from PubChem (https://pubchem.ncbi.nlm.nih.gov/) and the 3D structures of the other four effective compounds were obtained from TCMSP (https://www.tcmsp-e.com/). The JNK1 target protein was prepared for molecular docking simulations by adding hydrogens and removing water molecules and co-crystallized ligands. The position of the original ligand in the X-ray structure of JNK1 was defined as the binding site, and the energy of ligand binding to JNK1 was used to evaluate the binding ability. All docked positions were ranked using the affinity (kcal/mol) scoring function. The conformation with the lowest binding free energy was identified as the most probable binding mode. The results were visualized and analyzed using PyMOL v.3.0.1.

Statistical Analysis

All data were analyzed using IBM SPSS 22.0 software. Numerical values were expressed as mean ± standard error of the mean (S.E.M.). Statistical analyses were performed using one-way analysis of variance (ANOVA). If the variance was homogeneous, LSD method was performed. If the variance was inconsistent, the Dunnett's T3 test was performed. $P<0.05$ was considered statistically significant difference.

Results

ECC-BYF III Attenuated the Severity of Pulmonary Function and Inflammation in COPD Mice

Pulmonary function is an important indicator reflecting the condition of airflow limitation in COPD diagnosis. To evaluate the degree of pulmonary function, the WBP system was used to detect indicators of pulmonary function in mice. Compared with the control group, the indicators of TV, EF50, PEF and MVb were significantly decreased in the model group (Figure 2A–D). Indicators of TV, EF50, PEF, and MVb in the ECC-BYF III and NAC group, were significantly increased, compared with the model group (Figure 2A–D). These results suggested that ECC-BYF III could restore the decreased pulmonary function parameters and improve respiratory symptoms in COPD mice.

TNF-α, a pro-inflammatory cytokine, plays a key role in the airway inflammatory response in COPD.[14] Therefore, we measured the levels of TNF-α in serum and BALF using ELISA kits. The levels of TNF-α in the serum and BALF were significantly elevated in the model group than those in the control group (Figure 2E and F). After the administration of ECC-BYF III or NAC, the levels of TNF-α were markedly decreased in the serum and BALF compared with those in the model group. These results indicated that ECC-BYF III could significantly reduce the levels of TNF-α in the serum and BALF of COPD mice and alleviate the inflammatory response in the lung tissue.

ECC-BYF III Restored the Pulmonary Histopathology Changes in COPD Mice

Histopathological changes in the lung tissues of the different groups were observed using H&E staining. As shown in Figure 3A, the pulmonary alveolar structures of mice in the control group were fully intact with uniform size and space

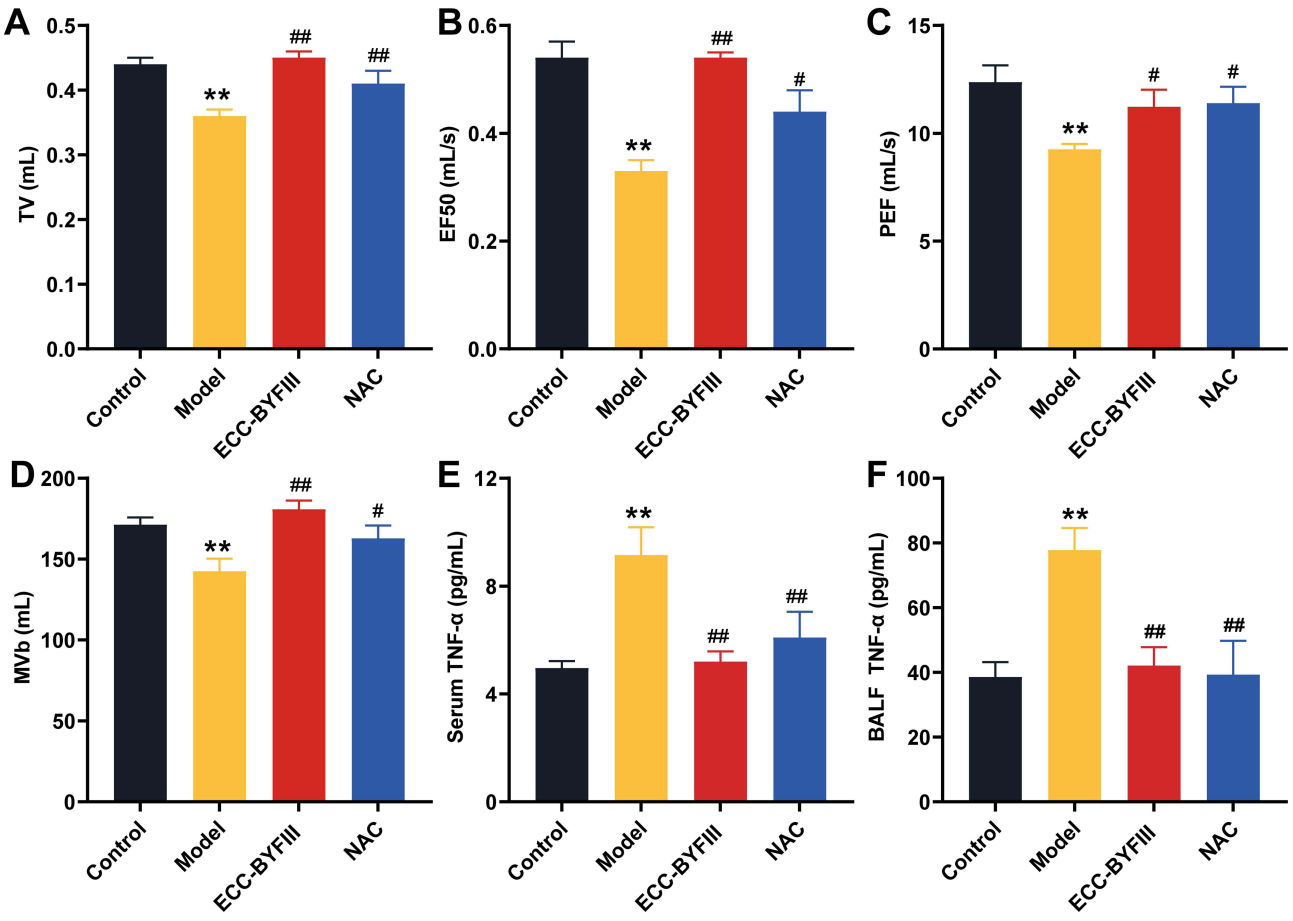

Figure 2 Effects of ECC-BYF III on the pulmonary function and inflammation in COPD mice. (**A**) Tidal volume. (**B**) 50% tidal volume expiratory flow. (**C**) Peak expiratory flow. (**D**) Minute volume. (**E** and **F**) The levels of TNF-α in the serum and BALF were detected by ELISA. Data are expressed as the mean ± SEM of three independent experiments (n=5,6). $^{**}P < 0.01$ versus control group. $^{\#}P < 0.05$, $^{\#\#}P < 0.01$ versus model group.

https://doi.org/10.2147/DDDT.S487074

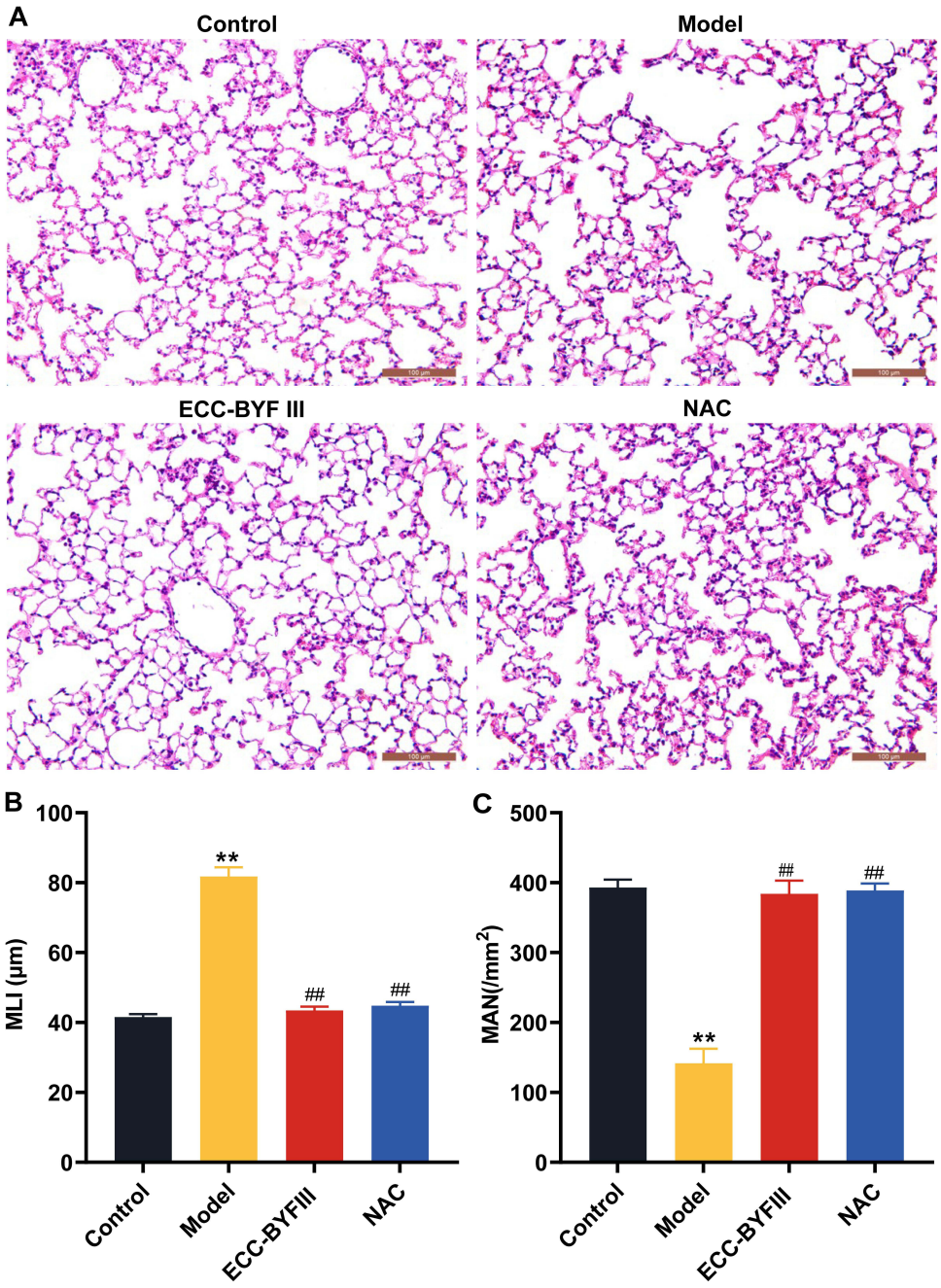

Figure 3 Effects of ECC-BYF III on histopathological changes in COPD mice. (**A**) Representative haematoxylin and eosin (HE) staining of lung samples. (**B**) Mean linear intercept. (**C**) Mean alveolar numbers. Data are expressed as the mean ± SEM of three independent experiments (n=5,6). $^{**}P < 0.01$ versus control group. $^{\#\#}P < 0.01$ versus model group.

of alveoli. Compared with the control group, the collapsed alveolar walls, irregularly enlarged and fused alveoli were observed in the lungs of the COPD mice. These pulmonary histopathological impairments were significantly ameliorated by ECC-BYF III and NAC treatments (Figure 3A). We then evaluated the mean alveolar number (MAN) and mean linear intercept (MLI) in the lung tissues (Figure 3B and C). Compared with the control group, the value of MAN was significantly decreased, while the MLI was increased in the model group. Treatment with ECC-BYF III and NAC increased the MAN value and decreased the MLI value compared with the model group. These results suggested that ECC-BYF III could improve the pulmonary histopathological changes in COPD mice.

https://doi.org/10.2147/DDDT.S487074

ECC-BYF III Improved Mitochondrial Ultrastructure in the Alveolar Epithelial Type II Cell of COPD Mice

Alveolar epithelial type II (AT2) cells are abundant in mitochondria to maintain lung function and high metabolism. Several studies have confirmed that CS could induce oxidative stress in AT2 cells, causing mitochondrial dysfunction or morphology alteration.[15] Therefore, we observed the mitochondrial ultrastructure in AT2 cells by electron microscopy (Figure 4). In the control group, normal mitochondria showed abundant cristae with an ordered arrangement. Whereas, mitochondrial ultrastructure of AT2 cells in the model group showed impaired mitochondria with swollen and disordered cristae. Compared with the model group, treatment with ECC-BYF III or NAC ameliorated mitochondrial swelling and cristae disorganization. Taken together, these results indicated that ECC-BYF III could improve mitochondrial fragmentation in COPD mice.

ECC-BYF III Alleviated Mitochondrial Dysfunction in COPD Mice

In addition to the morphological changes in the mitochondria, more indices of mitochondrial function were analyzed in the COPD mice. Mitochondrial membrane potential and mitochondrial respiratory chain complex I are important for maintaining mitochondrial function. We first examined the mitochondrial membrane potential using JC-1 dye. In healthy mitochondria, JC-1 is formed as aggregates in the mitochondrial matrix and emits red fluorescence. However, when the mitochondrial transmembrane potential is depolarized, JC-1 is formed as J-monomers which emits green fluorescence.[16] Compared with the control group, the percentage of red fluorescence was significantly reduced in the model group, indicating mitochondrial impairment (Figure 5A). Treatment with ECC-BYF III or NAC reversed the percentage of red fluorescence compared with that in the model group (Figure 5B). Next, we evaluated mitochondrial respiratory complex I in COPD mice using a mitochondrial respiratory chain complex activity assay kit (Figure 5C). Compared with the control group, the enzymatic activity of mitochondrial respiratory complex I was overtly inhibited in the mitochondria isolated from COPD mice. Treatment with ECC-BYF III and NAC significantly enhanced mitochondrial complex I activity, indicating that ECC-BYF III inhibited the decline of mitochondrial complex I activity in COPD mice. Taken together, these results suggested that ECC-BYF III could reverse mitochondrial function in COPD mice.

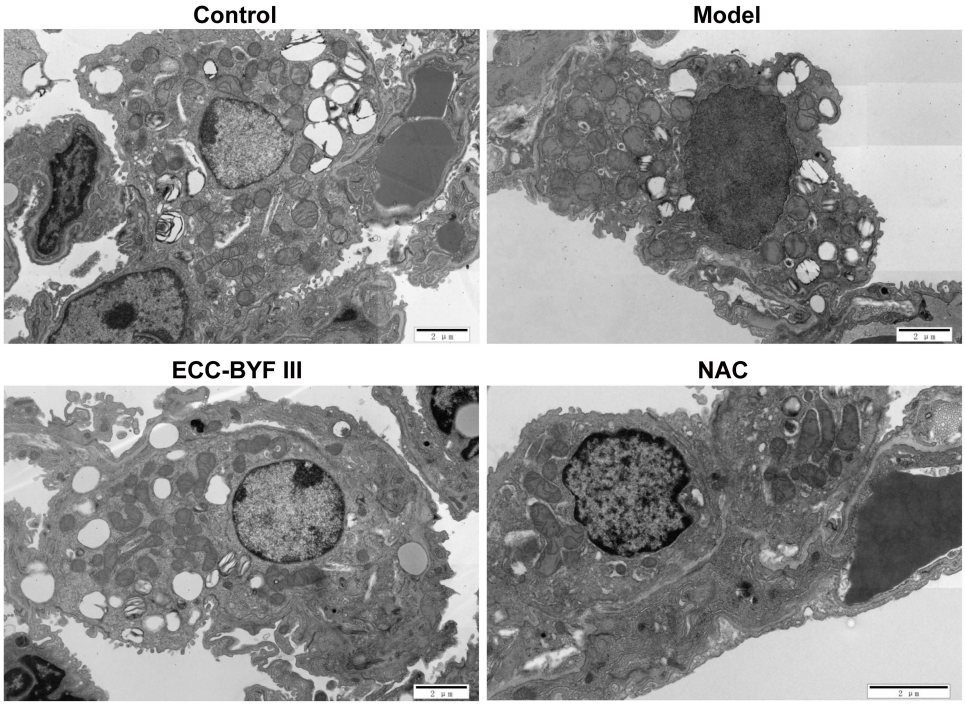

Figure 4 Effects of ECC-BYF III on Mitochondrial Ultrastructure in the AT2 of COPD mice.

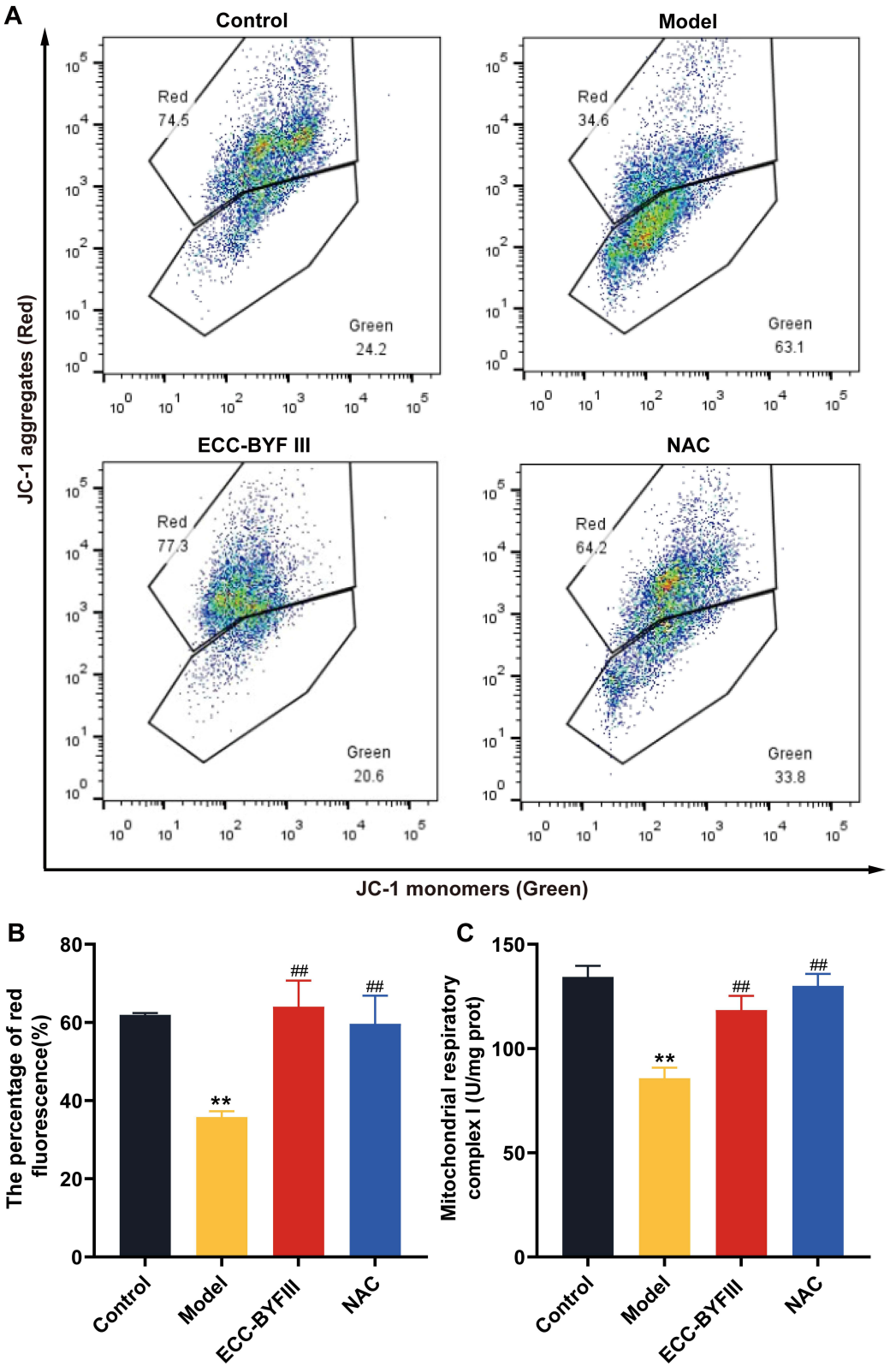

Figure 5 Effects of ECC-BYF III on mitochondrial function in COPD mice. (**A**) The mitochondrial membrane potential with JC-1 (n=3,4). (**B**) The percentage of red fluorescence. (**C**) Mitochondrial Complex I activity (n=5,6). Data are expressed as the mean ± SEM of three independent experiments. $^{**}P < 0.01$ versus control group. $^{\#\#}P < 0.01$ versus model group.

https://doi.org/10.2147/DDDT.S487074

ECC-BYF III Partially Rescued Mitochondrial Dysfunction of COPD Mice by Regulating JNK/Sab Pathway

As the JNK/Sab pathway has been reported to cause mitochondrial dysfunction under various stress conditions, we examined the impact of this pathway on the protective effects of ECC-BYF III in COPD mice. As shown in Figure 6, the protein levels of P-JNK and Sab were significantly higher in the lung tissues of COPD mice than those in the control group. ECC-BYF III or NAC could reverse the alterations of these protein levels. To determine the protective effects of ECC-BYF III on apoptosis, a consequence of mitochondrial dysfunction, we measured the level of the apoptotic executor protein cleaved CASP3 in COPD mice (Figure 6). As expected, the results showed that protein levels of cleaved CASP3 were significantly higher in the model group than in the control group. However, protein levels of cleaved CASP3 were obviously reduced in the ECC-BYF III and NAC groups compared with those in the model group (Figure 6). These results suggested that ECC-BYF III could hinder the activation of the JNK/Sab pathway, thereby mitigating mitochondrial dysfunction and apoptosis in the lung tissues of COPD mice.

Molecular Docking of JNK1 and Five Effective Compounds of ECC-BYF III

Molecular docking analysis is performed to evaluate the binding ability of the compounds and proteins. Typically, the binding energy below −5.0 kcal/mol indicates potential receptor-ligand interactions.[17] As shown in Figure 7, 20(S)-Ginsenoside Rh1

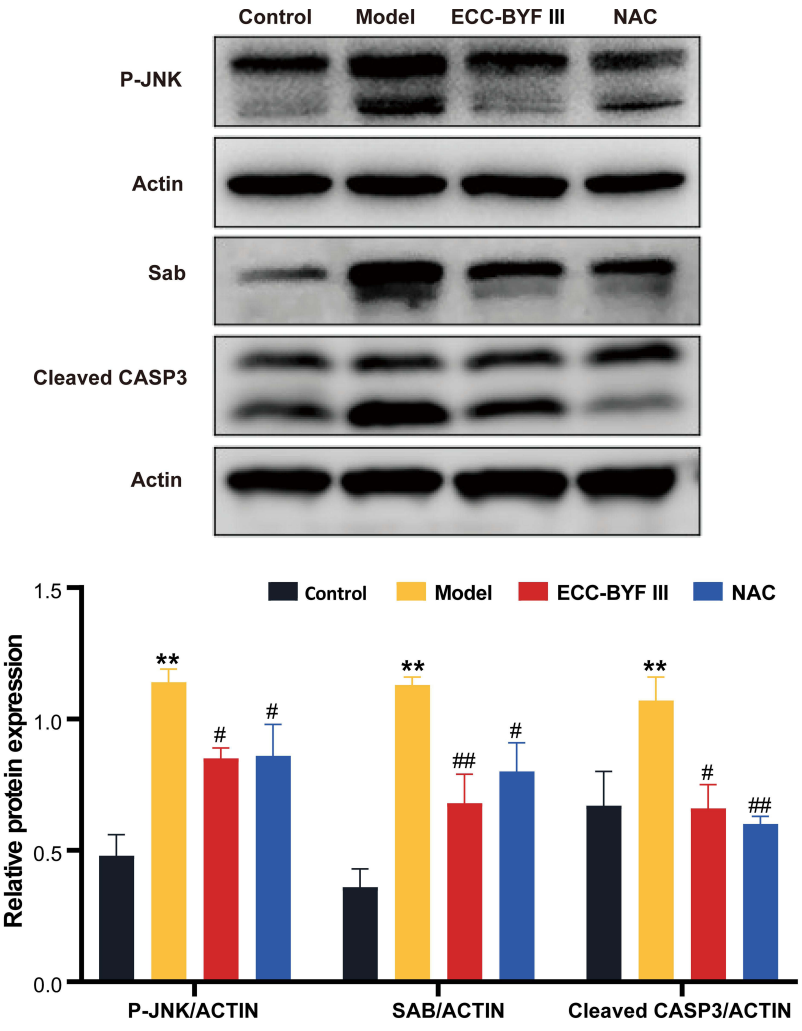

Figure 6 Effects of ECC-BYF III on JNK/Sab signaling pathway in COPD mice. The protein levels of P-JNK, Sab, and Cleaved CASP3 in the lungs of the different groups were evaluated by Western blotting. Data are expressed as the mean ± SEM of three independent experiments (n=3). $^{**}P < 0.01$ versus control group. $^{\#}P < 0.05$, $^{\#\#}P < 0.01$ versus the model group.

 https://doi.org/10.2147/DDDT.S487074

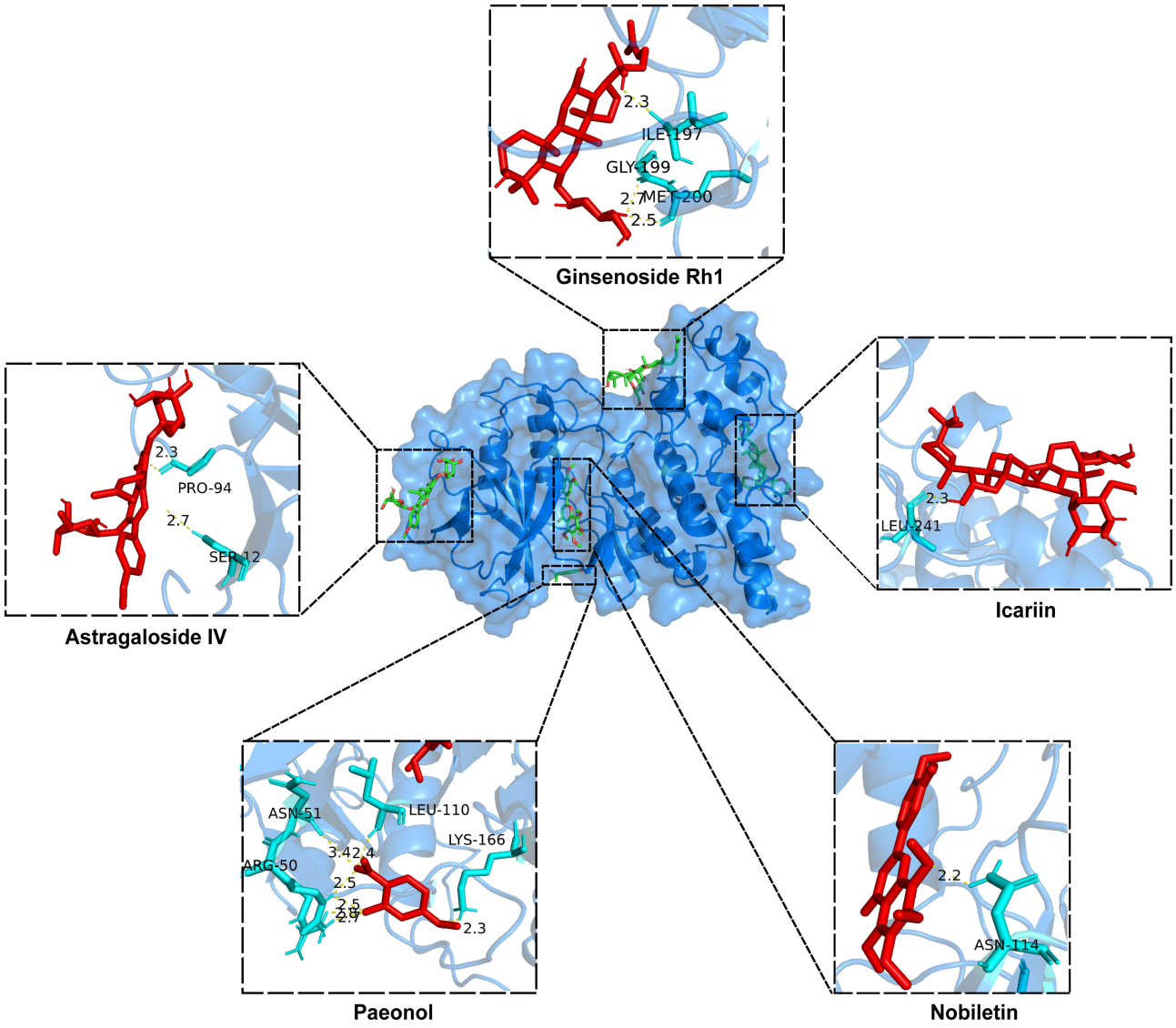

Figure 7 Molecular docking to predict the bindings of five effective compounds to JNK1 via AutoDock Vina and PyMOL. Demonstration of the predicted binding conformation and corresponding interaction amino acid residues of 20(S)-Ginsenoside Rh1, icariin, paeonol, nobiletin, and astragaloside IV docking into JNK1.

interacted with isoleucine (ILE)-197, glycine (GLY)-199, methionine (MET)-200 residues in JNK1 via hydrogen bonds. Icariin interacted with residues leucine (LEU)-241 in JNK1 via hydrogen bonds. Paeonol formed hydrogen bonds with amino acid residues asparagine (ASN)-51, LEU-110, lysine (LYS)-166, and arginine (ARG)-50 of JNK1. Nobiletin interacted with ASN-114 in JNK1 via hydrogen bonds. Similarly, astragaloside IV was connected to the proline (PRO)-94 and serine (SER)-12 residues of JNK1 through hydrogen bonds. Additionally, the binding energies of the five effective compounds and JNK1 were −15.07 kcal/mol, suggesting a significant binding affinity. These molecular docking results suggest the potential biological activities of ECC-BYF III on JNK protein, which might contribute to the inhibition of JNK/Sab pathway.

Discussion

COPD is one of the most common respiratory diseases that seriously threatens human health and the quality of life. However, the pathogenesis remains unclear. In this study, we demonstrated that ECC-BYF III could ameliorate pulmonary function, pulmonary histopathology, and inflammation in the COPD mice. Furthermore, ECC-BYF III played a protective role against mitochondrial dysfunction. This protective effect may be achieved by inhibiting the JNK/Sab pathway.

https://doi.org/10.2147/DDDT.S487074

Mitochondria are bilayer membrane organelles in eukaryotic cells that are able to provide energy to cells through oxidative phosphorylation and electron transport.[18] Dysfunctional mitochondria induce the release of large amounts of ROS from adjacent mitochondria, which could further lead to cell death.[19] Clinical research showed that an increase in mtROS, as well as a decrease in mitochondrial membrane potential, were observed in mitochondria isolated from bronchial biopsies of COPD patients.[20] Furthermore, recent studies demonstrated that mitochondrial dysfunction was present in alveolar epithelial cells of both COPD patients and mice.[21,22] These results indicated that mitochondrial dysfunction played an important role in the pathogenesis of COPD. In our study, COPD mice exhibited severe structural and functional changes in mitochondria, as confirmed by mitochondrial swelling, cristae disorganization, decreased MMP and enzymatic activity of mitochondrial respiratory complex I. Meanwhile, ECC-BYF III administration not only improved the structure and numbers of mitochondria, but also restored MMP and enzymatic activity of mitochondrial respiratory complex I. These results demonstrated that ECC-BYF III could inhibit mitochondrial dysfunction and COPD development, providing new insights into the treatment of COPD.

Sustained JNK activation plays an important role in mitochondrial dysfunction in COPD. JNK, a member of the mitogen-activated protein kinase (MAPK) family, is a stress-activated protein kinase.[23] According to a clinical study, COPD patients showed a higher P-JNK expression in their lung epithelial cells.[24] However, the potential role of P-JNK in the pathogenesis of COPD is still unclear. In recent years, researchers found that activated JNK could bind to a mitochondrial surface membrane protein (Sab) and then migrate to mitochondria, disrupting the electron transport chain and promoting the release of ROS, ultimately leading to hepatocyte death during liver injury.[25] Furthermore, previous studies have confirmed that inhibition of JNK/Sab interaction could hinder JNK-mitochondrial signaling and alleviate 6-hydroxydopamine-induced oxidative stress, mitochondrial dysfunction and neurotoxicity.[26] A similar study also found that preventing P-JNK from binding to Sab attenuated mitochondrial dysfunction in cardiomyocytes and ischemic necrosis in the rat heart.[27] In addition, Chambers et al found that inhibition of Sab-related signaling could suppress oxidative stress, mitochondrial dysfunction, and apoptosis of cardiomyocytes mediated by imatinib mesylate, whereas overexpressing Sab enhances the cardiotoxicity of imatinib mesylate.[28] In the lung, aberrant activation of the JNK-mitochondria pathway could significantly disrupt the physiological function of lung cells, leading to acute lung injury and acute respiratory distress syndrome (ALI/ARDS). Whereas, selective inhibition of JNK signaling on mitochondria protected against mitochondrial dysfunction and cell death induced by lipopolysaccharide (LPS) in ALI/ARDS mice.[29] In comparison with previous studies, our results showed that the expression of P-JNK and Sab proteins were up-regulated in the lung tissues of COPD mice, along with inflammation, mitochondrial dysfunction and apoptosis. Our results also showed that ECC-BYF III had an inhibitory effect on the JNK/Sab pathway in COPD mice, as evidenced by the decreased levels of P-JNK and Sab proteins.

The interaction between P-JNK and Sab increases superoxide production in mitochondria, leading to apoptosis via outer mitochondrial membrane permeabilization.[30] Apoptosis is a self-destructive process in cell life cycle that occurs during cell development, tissue repair, or disease states. Mitochondria are important regulatory centers of apoptosis pathways.[31] As mitochondrial dysfunction occurs, apoptosis-related factors are released from the mitochondria into the cytoplasm, activating downstream proteins of the cysteinyl aspartate-specific proteinase (Caspase) family and triggering cell apoptosis. Cleaved caspase-3 (CASP3), a biomarker of apoptosis, is a crucial executioner of apoptosis.[32] To further explore the anti-apoptotic mechanism of ECC-BYF III, the expression of cleaved CASP3 were assessed. Our results demonstrated that apoptosis was increased in the lung of COPD mice compared with that in the control group, and treatment with ECC-BYF III reduced apoptosis.

In summary, ECC-BYF III improved the pulmonary function, histopathology, and inflammation. Reduction in mitochondrial membrane potential and mitochondrial complex I activity, as well as changes in mitochondrial numbers and morphology in the lung tissues of COPD mice, were reversed by ECC-BYF III treatment. There results indicated that the protective effects of ECC-BYF III were attributed to improving mitochondrial function. Moreover, our study showed that ECC-BYF III treatment decreased the levels of P-JNK, Sab and cleaved CASP3. Molecular docking analysis results demonstrated that five effective compounds of ECC-BYF III have high binding affinities with JNK1 protein. Taken together, we conclude that ECC-BYF III partially ameliorates mitochondrial dysfunction in COPD by inhibiting the JNK/Sab pathway.

Conclusion

Our study demonstrated the therapeutic effects of ECC-BYF III in COPD mice. ECC-BYF III treatment protected against COPD by improving mitochondrial dysfunction and apoptosis, which was attributed to inhibition of the JNK/Sab pathway. Collectively, ECC-BYF III showed great potential as a preventive and therapeutic drug for mitochondrial dysfunction in COPD. Nonetheless, it is worth to note that our study did not use gene silencing or inhibitors experiments focusing on the JNK/Sab pathway. In further, we need to further explore the detail mechanism of ECC-BYF III on JNK/Sab signaling by vitro experiments.

Data Sharing Statement

The original contributions presented in the study are included in the article. Further inquiries can be directed to the corresponding authors.

Informed Consent Statement

All animal protocols were performed in accordance with the Guidelines for Animal Experimentation and were approved by the Animal Ethics Committee of Henan University of Chinese Medicine (approval no. DWLL201903072). We complied with the provisions of national standard "Laboratory animal-Guideline for ethical review of animal welfare (GB/T 35892-2018)" to ensure the welfare of the experimental animals used in our research.

Funding

This work was partially supported by the National Natural Science Foundation of China (81904033, 82074406), Foundation of Science and Technology Department of HeNan Province (232102311215), and the China Postdoctoral Science Foundation (2020M672244).

Disclosure

The authors report no conflicts of interest in this work.

References

1. Global Initiative for Chronic Obstructive Lung Disease. Global strategy for the diagnosis, management, and prevention of chronic obstructive pulmonary disease. 2025. Available from: https://goldcopd.org. Accessed January 8, 2025.
2. Barnes PJ. Oxidative stress in chronic obstructive pulmonary disease. *Antioxidants*. 2022;11(5):965. doi:10.3390/antiox11050965
3. World Health Organization. Tobacco and Chronic Obstructive Pulmonary Disease (COPD), WHO Tobacco Knowledge Summaries. 2023. Available from: https://www.who.int/publications/i/item/9789240084452. Accessed January 15, 2025.
4. Jiang Y, Wang X, Hu D. Mitochondrial alterations during oxidative stress in chronic obstructive pulmonary disease. *Int J Chron Obstruct Pulmon Dis*. 2017;12:1153–1162. doi:10.2147/copd.S130168
5. Barnes PJ. Oxidative stress-based therapeutics in COPD. *Redox Biol*. 2020;33:101544. doi:10.1016/j.redox.2020.101544
6. van der Toorn M, Slebos DJ, de Bruin HG, et al. Cigarette smoke-induced blockade of the mitochondrial respiratory chain switches lung epithelial cell apoptosis into necrosis. *Am J Physiol Lung Cell Mol Physiol*. 2007;292(5):L1211–L1218. doi:10.1152/ajplung.00291.2006
7. Hara H, Araya J, Ito S, et al. Mitochondrial fragmentation in cigarette smoke-induced bronchial epithelial cell senescence. *Am J Physiol Lung Cell Mol Physiol*. 2013;305(10):L737–L746. doi:10.1152/ajplung.00146.2013
8. Win S, Than TA, Han D, Petrovic LM, Kaplowitz N. c-Jun N-terminal kinase (JNK)-dependent acute liver injury from Acetaminophen or tumor necrosis factor (TNF) requires mitochondrial Sab protein expression in mice. *J Biol Chem*. 2011;286(40):35071–35078. doi:10.1074/jbc.M111.276089
9. Jiang Y, Xu J, Huang P, et al. Scoparone improves nonalcoholic steatohepatitis through alleviating JNK/Sab signaling pathway-mediated mitochondrial dysfunction. *Front Pharmacol*. 2022;13:863756. doi:10.3389/fphar.2022.863756
10. Li K, Mei X, Xu K, et al. Comparative study of cigarette smoke, Klebsiella pneumoniae, and their combination on airway epithelial barrier function in mice. *Environ Toxicol*. 2023;38(5):1133–1142. doi:10.1002/tox.23753
11. Wang M, Li J, Li S, Xie Y. Effects of comprehensive therapy based on traditional Chinese medicine patterns on older patients with chronic obstructive pulmonary disease: a subgroup analysis from a four-center, randomized, controlled study. *Front Med*. 2014;8(3):368–375. doi:10.1007/s11684-014-0360-0
12. Li J, Liu X, Dong H, et al. Effective-constituent compatibility-based analysis of Bufei Yishen formula, a traditional herbal compound as an effective treatment for chronic obstructive pulmonary disease. *J Integr Med*. 2020;18(4):351–362. doi:10.1016/j.joim.2020.04.004
13. Jin F, Zhang L, Chen K, et al. Effective-component compatibility of Bufei Yishen formula III combined with electroacupuncture suppresses inflammatory response in rats with chronic obstructive pulmonary disease via regulating SIRT1/NF-κB signaling. *Biomed Res Int*. 2022;2022:3360771. doi:10.1155/2022/3360771

14. Guo P, Li R, Piao TH, Wang CL, Wu XL, Cai HY. Pathological mechanism and targeted drugs of COPD. *Int J Chron Obstruct Pulmon Dis*. 2022;17:1565–1575. doi:10.2147/copd.S366126
15. Aghapour M, Remels AHV, Pouwels SD, et al. Mitochondria: at the crossroads of regulating lung epithelial cell function in chronic obstructive pulmonary disease. *Am J Physiol Lung Cell Mol Physiol*. 2020;318(1):L149–L164. doi:10.1152/ajplung.00329.2019
16. Elefantova K, Lakatos B, Kubickova J, Sulova Z, Breier A. Detection of the mitochondrial membrane potential by the cationic dye JC-1 in L1210 cells with massive overexpression of the plasma membrane ABCB1 drug transporter. *Int J Mol Sci*. 2018;19(7):1985. doi:10.3390/ijms19071985
17. Cao X, Li G, Xie J, et al. Screening antioxidant components in different parts of dandelion using online gradient pressure liquid extraction coupled with high-performance liquid chromatography antioxidant analysis system and molecular simulations. *Molecules*. 2024;29(10):2315. doi:10.3390/molecules29102315
18. Vinten-Johansen J. Commentary: mitochondria are more than just the cells' powerhouse. *J Thorac Cardiovasc Surg*. 2020;160(2):e33–e34. doi:10.1016/j.jtcvs.2019.07.029
19. Peng W, Cai G, Xia Y, et al. Mitochondrial dysfunction in Atherosclerosis. *DNA Cell Biol*. 2019;38(7):597–606. doi:10.1089/dna.2018.4552
20. Wiegman CH, Michaeloudes C, Haji G, et al. Oxidative stress-induced mitochondrial dysfunction drives inflammation and airway smooth muscle remodeling in patients with chronic obstructive pulmonary disease. *J Allergy Clin Immunol*. 2015;136(3):769–780. doi:10.1016/j.jaci.2015.01.046
21. Carraway MS, Suliman HB, Kliment C, Welty-Wolf KE, Oury TD, Piantadosi CA. Mitochondrial biogenesis in the pulmonary vasculature during inhalational lung injury and fibrosis. *Antioxid Redox Signal*. 2008;10(2):269–275. doi:10.1089/ars.2007.1910
22. Kosmider B, Lin CR, Karim L, et al. Mitochondrial dysfunction in human primary alveolar type II cells in emphysema. *EBioMedicine*. 2019;46:305–316. doi:10.1016/j.ebiom.2019.07.063
23. Ryter SW, Rosas IO, Owen CA, et al. Mitochondrial dysfunction as a pathogenic mediator of chronic obstructive pulmonary disease and idiopathic pulmonary fibrosis. *Ann Am Thorac Soc*. 2018;15(Suppl 4):S266–S272. doi:10.1513/AnnalsATS.201808-585MG
24. Eurlings IM, Reynaert NL, van de Wetering C, et al. Involvement of c-Jun N-Terminal kinase in TNF-α-driven remodeling. *Am J Respir Cell Mol Biol*. 2017;56(3):393–401. doi:10.1165/rcmb.2015-0195OC
25. Win S, Than TA, Min RW, Aghajan M, Kaplowitz N. c-Jun N-terminal kinase mediates mouse liver injury through a novel Sab (SH3BP5)-dependent pathway leading to inactivation of intramitochondrial Src. *Hepatology*. 2016;63(6):1987–2003. doi:10.1002/hep.28486
26. Chambers JW, Howard S, LoGrasso PV. Blocking c-Jun N-terminal kinase (JNK) translocation to the mitochondria prevents 6-hydroxydopamine-induced toxicity in vitro and in vivo. *J Biol Chem*. 2013;288(2):1079–1087. doi:10.1074/jbc.M112.421354
27. Chambers JW, Pachori A, Howard S, Iqbal S, LoGrasso PV. Inhibition of JNK mitochondrial localization and signaling is protective against ischemia/reperfusion injury in rats. *J Biol Chem*. 2013;288(6):4000–4011. doi:10.1074/jbc.M112.406777
28. Chambers TP, Santiesteban L, Gomez D, Chambers JW. Sab mediates mitochondrial dysfunction involved in imatinib mesylate-induced cardiotoxicity. *Toxicology*. 2017;382:24–35. doi:10.1016/j.tox.2017.03.006
29. Li C, Ma D, Chen Y, Liu W, Jin F, Bo L. Selective inhibition of JNK located on mitochondria protects against mitochondrial dysfunction and cell death caused by endoplasmic reticulum stress in mice with LPS-induced ALI/ARDS. *Int J Mol Med*. 2022;49(6):85. doi:10.3892/ijmm.2022.5141
30. Win S, Than TA, Kaplowitz N. Mitochondrial P-JNK target, SAB (SH3BP5), in regulation of cell death. *Front Cell Dev Biol*. 2024;12:1359152. doi:10.3389/fcell.2024.1359152
31. Li CL, Liu JF, Liu SF. Mitochondrial dysfunction in chronic obstructive pulmonary disease: unraveling the molecular nexus. *Biomedicines*. 2024;12(4):814. doi:10.3390/biomedicines12040814
32. Eskandari E, Eaves CJ. Paradoxical roles of caspase-3 in regulating cell survival, proliferation, and tumorigenesis. *J Cell Biol*. 2022;221(6):e202201159. doi:10.1083/jcb.202201159